CBI-TMI: Synthesis and Evaluation of a Key Analog of the Duocarmycins. Validation of a Direct Relationship between Chemical Solvolytic Stability and Cytotoxic Potency and Confirmation of the Structural Features Responsible for the Distinguishing Behavior of Enantiomeric Pairs of Agents

Dale L. Boger* and Weiya Yun

Contribution from the Department of Chemistry, The Scripps Research Institute, 10666 North Torrey Pines Road, La Jolla, California 92037

*Received March 21, 1994**

Abstract: The synthesis of (+)- and *ent*-(-)-CBI-TMI (**3**), a key analog of the naturally occurring potent antitumor antibiotics duocarmycin SA (**1**) and duocarmycin A (**2**), is disclosed and was facilitated by the development of a general and direct chromatographic resolution of the advanced synthetic intermediate **13** on a preparative Diacel Chiralcel OD HPLC column. The DNA alkylation properties and the cytotoxic activity of (+)- and (-)-CBI-TMI (**3**) are detailed in conjunction with a comparative study of a key series of duocarmycin SA and A analogs. (+)-CBI-TMI proved to be an effective DNA alkylating agent which exhibited a selectivity and efficiency of DNA alkylation that are not distinguishable from those of (+)-duocarmycin SA (**1**), and it was found to be an exceptionally potent cytotoxic agent (IC_{50} = 30 pM, L1210). The comparative examination of the natural enantiomers of duocarmycin SA (**1**), duocarmycin A (**2**), CBI-TMI (**3**), and CI-TMI (**4**) revealed that the agents follow a predictable linear relationship between solvolytic chemical stability and cytotoxic activity which spans 3–4 orders of magnitude for the series of agents examined. In contrast, *ent*-(-)-CBI-TMI, unlike *ent*-(-)-duocarmycin SA, exhibited less effective DNA alkylation properties (100×) and it proved to be a relatively nonpotent cytotoxic agent (100×). These latter observations are consistent with expectations based on recent models advanced which suggest that the distinguishing behavior of such unnatural enantiomers is the result of destabilizing steric interactions surrounding the duocarmycin C7 center.

Two independent efforts have described the isolation, structure determination and preliminary evaluation of the initial members of a new class of exceptionally potent antitumor antibiotics including duocarmycin A (**2**),[1-3] duocarmycin B_1-B_2,[5] duocarmycin C_1-C_2[2-4] (pyrindamycin B and A),[6] and duocarmycin SA (**1**).[7] Subsequent to their disclosure, we described the event,[8] sequence selectivity,[9] quantitation,[10] reversibility,[11] and unambiguous establishment of the structure[10] of the adenine N3 DNA alkylation reaction for duocarmycin A and C_1-C_2, which provided the necessary information for development of an accurate model[9,12,13] of the predominant DNA alkylation event. In these studies, the major DNA alkylation reaction (86–92%) was shown to proceed by 3′ adenine N3 addition to the less substituted cyclopropane carbon preferentially within selected, four base-pair AT-rich minor groove sites (5′-AAA > 5′-TTA ≫ 5′-TAA > 5′-ATA) with an agent binding orientation in the minor groove that extends in the 3′ → 5′ direction from the site of alkylation covering 3.5 base pairs. In these studies, the reactive agents incorporating the pharmacophore of the duocarmycin alkylation subunit including CI-TMI (**4**) and *N*-BOC-CI (**9**) were prepared and examined.[8,9] Unlike the observations made with CI-TMI, a subsequent comparative examination of (+)-duocarmycin A (**2**) with *epi*-(+)-duocarmycin A and their unnatural enantiomers[14] revealed that the productive DNA alkylation properties were embodied in the natural enantiomers (≥100× more effective) and that *epi*-(+)-duocarmycin A exhibited the same sequence selectivity as (+)-duocarmycin A but a diminished DNA alkylation efficiency (3–6×).[15] The recent demonstration that sensitive cell lines undergo induced apoptotic cell death upon treatment with (+)-duocarmycin SA at therapeutically relevant doses has provided the first characterizable link between DNA alkylation and the productive antitumor properties of the agents.[16]

* Abstract published in *Advance ACS Abstracts,* August 1, 1994.

(1) Duocarmycin A: Takahashi, I.; Takahashi, K.; Ichimura, M.; Morimoto, M.; Asano, K.; Kawamoto, I.; Tomita, F.; Nakano, H. *J. Antibiot.* **1988**, *41*, 1915.

(2) Yasuzawa, T.; Iida, T.; Muroi, K.; Ichimura, M.; Takahashi, K.; Sano, H. *Chem. Pharm. Bull.* **1988**, *36*, 3728.

(3) Duocarmycin C_l and duocarmycin A: Nakano, H.; Takahashi, I.; Ichimura, M.; Kawamoto, I.; Asano, K.; Tomita, F.; Sano, H.; Yasuzawa, T.; Morimoto, M.; Fujimoto, K. PCT. Int. Appl. WO87 06265, 1987; *Chem. Abstr.* **1988**, *108*, 110858s.

(4) Duocarmycin C_l: Ichimura, M.; Muroi, K.; Asano, K.; Kawamoto, I.; Tomita, F.; Morimoto, M.; Nakano, H. *J. Antibiot.* **1988**, *41*, 1285.

(5) Duocarmycin B_1 and B_2: Ogawa, T.; Ichimura, M.; Katsumata, S.; Morimoto, M.; Takahashi, K. *J. Antibiot.* **1989**, *42*, 1299.

(6) Pyrindamycin A and B: Ohba, K.; Watabe, H.; Sasaki, T.; Takeuchi, Y.; Kodama, Y.; Nakazawa, T.; Yamamoto, H.; Shomura, T.; Sezaki, M.; Kondo, S. *J. Antibiot.* **1988**, *41*, 1515. Ishii, S.; Nagasawa, M.; Kariya, Y.; Yamamoto, H.; Inouye, S.; Kondo, S. *J. Antibiot.* **1989**, *42*, 1713.

(7) Ichimura, M.; Ogawa, T.; Takahashi, K.; Kobayashi, E.; Kawamoto, I.; Yasuzawa, T.; Takahashi, I.; Nakano, H. *J. Antibiot.* **1990**, *43*, 1037. Ichimura, M.; Ogawa, T.; Katsumata, S.; Takahashi, K.; Takahashi, I.; Nakano, H. *J. Antibiot.* **1991**, *44*, 1045.

(8) Boger, D. L.; Ishizaki, T.; Zarrinmayeh, H.; Kitos, P. A.; Suntornwat, O. *J. Org. Chem.* **1990**, *55*, 4499.

(9) Boger, D. L.; Ishizaki, T.; Zarrinmayeh, H.; Munk, S. A.; Kitos, P. A.; Suntornwat, O. *J. Am. Chem. Soc.* **1990**, *112*, 8961.

(10) Boger, D. L.; Ishizaki, T.; Zarrinmayeh, H. *J. Am. Chem. Soc.* **1991**, *113*, 6645.

(11) Boger, D. L.; Yun, W. *J. Am. Chem. Soc.* **1993**, *115*, 9872.

(12) (a) Boger, D. L. *Chemtracts: Org. Chem.* **1991**, *4*, 329. (b) Boger, D. L. In *Advances in Heterocyclic Natural Products Synthesis;* Pearson, W. H., Ed.; JAI Press: Greenwich, CT, 1992; Vol. 2, pp 1–188.

(13) Boger, D. L. *Proc. Robert A. Welch Found. Conf. Chem. Res., XXXV. Chem. Front. Med.* **1991**, *35*, 137.

(14) Boger, D. L.; Yun, W.; Terashima, S.; Fukuda, Y.; Nakatani, K.; Kitos, P. A.; Jin, Q. *Bioorg. Med. Chem. Lett.* **1992**, *2*, 759. For the total synthesis of duocarmycin A: Fukuda, Y.; Nakatani, K.; Terashima, S. *Bioorg. Med. Chem. Lett.* **1992**, *2*, 755. Fukuda, Y.; Nakatani, K.; Ito, Y.; Terashima, S. *Tetrahedron Lett.* **1990**, *31*, 6699.

(15) For related studies, see: Sugiyama, H.; Hosoda, M.; Saito, I.; Asai, A.; Saito, H. *Tetrahedron Lett.* **1990**, *31*, 7197. Lin, C. H.; Patel, D. J. *J. Am. Chem. Soc.* **1992**, *114*, 10658. Sugiyama, H.; Ohmori, K.; Chan, K. L.; Hosoda, M.; Asai, A.; Saito, H.; Saito, I. *Tetrahedron Lett.* **1993**, *34*, 2179. Yamamoto, K.; Sugiyama, H.; Kawanishi, S. *Biochemistry* **1993**, *32*, 1059.

0002-7863/94/1516-7996$04.50/0

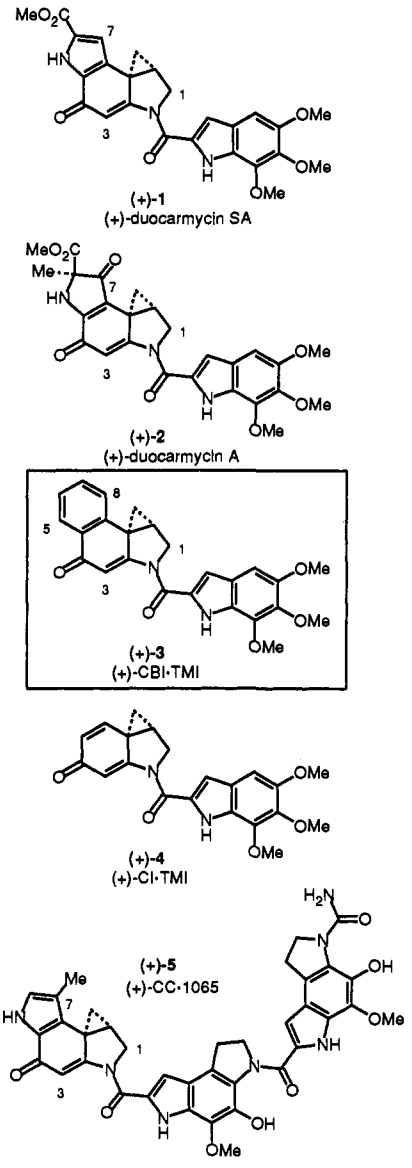

More recently, we reported a detailed study[17] of the DNA alkylation properties of (+)-duocarmycin SA (**1**), *ent*-(−)-duocarmycin SA, and both enantiomers of *N*-BOC-DSA (**6**), a simple derivative of the alkylation subunit.[18] In addition to the first disclosure of the event, sequence selectivity, quantitation, reversibility, and structural confirmation of the minor groove adenine N3 alkylation by natural (+)-duocarmycin SA, the studies constituted the first disclosure of DNA alkylation by a duocarmycin unnatural enantiomer. For *ent*-(−)-duocarmycin SA, the DNA alkylation reaction was shown to proceed by 5′ adenine N3 addition to the least substituted cyclopropane carbon preferentially within selected, four base pair AT-rich minor groove sites (5′-AAA > 5′-AAT > 5′-TAA > 5′-TAT) with an agent binding orientation that extends in the reverse 5′ → 3′ direction. As a consequence of the diastereomeric relationship of the enantiomer adducts, the unnatural enantiomer binding starts at the 5′ base preceding the alkylation site and extends in the 5′ direction across the adenine alkylation site and the adjacent 1–2 bases to the 3′ side of adenine alkylation site. The beauty and accuracy of the model revealed itself when it provided an attractive explanation for the unusual observation that both enantiomers of **6**, (+)- and *ent*-(−)-*N*-BOC-DSA, alkylate the same sites in DNA with the identical sequence selectivity (5′-AA > 5′-TA) resulting from the diastereomeric nature of the adducts. Inherent in this work was the verification of the prominent role that noncovalent binding selectivity[19] plays in contributing to the sequence selective DNA alkylation reactions of the natural products. Because of the enhanced solvolytic stability[18] and biological potency[17,18] of (+)-duocarmycin SA (**1**) relative to its predecessors including (+)-duocarmycin A (**2**), (+)-CC-1065 (**5**),[11,20-24] and structurally related agents,[24-27] the examination of (+)-**1**, its unnatural enantiomer, and the structurally related agents (+)- and *ent*-(−)-**6** proved to be especially informative.

On the basis of the models developed in the course of this work which explain the origin of the offset AT-rich alkylation selectivity of enantiomeric pairs of agents,[17,23] an attractive explanation for the apparently confusing and distinguishing behavior of pairs of

(16) Boger, D. L.; Johnson, D. S.; Wrasidlo, W. *Bioorg. Med. Chem. Lett.* **1994**, *4*, 631.

(17) Boger, D. L.; Johnson, D. S.; Yun, W. *J. Am. Chem. Soc.* **1994**, *116*, 1635.

(18) Boger, D. L.; Machiya, K.; Hertzog, D. L.; Kitos, P. A.; Holmes, D. *J. Am. Chem. Soc.* **1993**, *115*, 9025. Boger, D. L.; Machiya, K. *J. Am. Chem. Soc.* **1992**, *114*, 10056. Boger, D. L. *Pure Appl. Chem.* **1993**, *65*, 1123.

(19) Boger, D. L.; Invergo, B. J.; Coleman, R. S.; Zarrinmayeh, H.; Kitos, P. A.; Thompson, S. C.; Leong, T.; McLaughlin, L. W. *Chem.-Biol. Interact.* **1990**, *73*, 29. Boger, D. L.; Sakya, S. M. *J. Org. Chem.* **1992**, *57*, 1277. Boger, D. L.; Coleman, R. S.; Invergo, B. J. *J. Org. Chem.* **1987**, *52*, 1521. Boger, D. L.; Coleman, R. S. *J. Org. Chem.* **1984**, *49*, 2240.

(20) Warpehoski, M. A. In *Advances in DNA Sequence Specific Agents*; Hurley, L. H., Ed.; JAI Press: Greenwich, CT, 1992; Vol. 1, p 217. Warpehoski, M. A.; Hurley, L. H. *Chem. Res. Toxicol.* **1988**, *1*, 315. Hurley, L. H.; Draves, P. H. In *Molecular Aspects of Anticancer Drug-DNA Interactions*; Neidle, S., Waring, M., Eds.; CRC Press: Ann Arbor, MI, 1993; Vol. 1, p 89. Hurley, L. H.; Needham-VanDevanter, D. R. *Acc. Chem. Res.* **1986**, *19*, 230.

(21) Coleman, R. S.; Boger, D. L. In *Studies in Natural Product Chemistry*; Rahman, A.-u, Ed.; Elsevier: Amsterdam, The Netherlands, 1989; Vol. 3, p 301.

(22) Hurley, L. H.; Warpehoski, M. A.; Lee, C.-S.; McGovren, J. P.; Scahill, T. A.; Kelly, R. C.; Mitchell, M. A.; Wicnienski, N. A.; Gebhard, I.; Johnson, P. D.; Bradford, V. S. *J. Am. Chem. Soc.* **1990**, *112*, 4633. Wierenga, W.; Bhuyan, B. K.; Kelly, R. C.; Krueger, W. C.; Li, L. H.; McGovren, J. P.; Swenson, D. H.; Warpehoski, M. A. *Adv. Enzyme Regul.* **1986**, *25*, 141. Warpehoski, M. A.; Gebhard, I.; Kelly, R. C.; Krueger, W. C.; Li, L. H.; McGovren, J. P.; Prairie, M. D.; Wicnienski, N.; Wierenga, W. *J. Med. Chem.* **1988**, *31*, 590. See also refs 11 and 12. Synthesis of CPI subunit, see: Wierenga, W. *J. Am. Chem. Soc.* **1981**, *103*, 5621. Magnus, P.; Gallagher, T.; Schultz, J.; Or, Y.-S.; Ananthanarayan, T. P. *J. Am. Chem. Soc.* **1987**, *109*, 2706. Kraus, G. A.; Yue, S.; Sy, J. *J. Org. Chem.* **1985**, *50*, 283. Boger, D. L.; Coleman, R. S. *J. Am. Chem. Soc.* **1988**, *110*, 1321, 4796. Bolton, R. E.; Moody, C. J.; Pass, M.; Rees, C. W.; Tojo, G. *J. Chem. Soc., Perkin Trans. 1* **1988**, 2491. Sundberg, R. J.; Baxter, E. W.; Pitts, W. J.; Ahmed-Schofield, R.; Nishiguchi, T. *J. Org. Chem.* **1988**, *53*, 5097. Sundberg, R. J.; Pitts, W. J. *J. Org. Chem.* **1991**, *56*, 3048. Martin, P. *Helv. Chim. Acta* **1989**, *72*, 1554. Toyota, M.; Fukumoto, K. *J. Chem. Soc., Perkin Trans. 1* **1992**, 547. Tietze, L. F.; Grote, T. *J. Org. Chem.* **1994**, *59*, 192.

(23) Boger, D. L.; Johnson, D. S.; Yun, W.; Tarby, C. M. *Bioorg. Med. Chem.* **1994**, *2*, 115. Boger, D. L.; Coleman, R. S.; Invergo, B. J.; Sakya, S. M.; Ishizaki, T.; Munk, S. A.; Zarrinmayeh, H.; Kitos, P. A.; Thompson, S. C. *J. Am. Chem. Soc.* **1990**, *112*, 4623. Boger, D. L.; Coleman, R. S. *J. Am. Chem. Soc.* **1988**, *110*, 4796 and 1321.

(24) Boger, D. L.; Munk, S. A.; Zarrinmayeh, H.; Ishizaki, T.; Haught, J.; Bina, M. *Tetrahedron* **1991**, *47*, 2661.

(25) CI-based analogs: Boger, D. L.; Zarrinmayeh, H.; Munk, S. A.; Kitos, P. A.; Suntornwat, O. *Proc. Natl. Acad. Sci. U.S.A.* **1991**, *88*, 1431. Boger, D. L.; Munk, S. A.; Zarrinmayeh, H. *J. Am. Chem. Soc.* **1991**, *113*, 3980. Synthesis: Boger, D. L.; Wysocki, R. J., Jr. *J. Org. Chem.* **1989**, *54*, 1238. Boger, D. L.; Wysocki, R. J.; Jr.; Ishizaki, T. *J. Am. Chem. Soc.* **1990**, *112*, 5230. Drost, K. J.; Jones, R. J.; Cava, M. P. *J. Org. Chem.* **1989**, *54*, 5985. Tidwell, J. H.; Buchwald, S. L. *J. Org. Chem.* **1992**, *57*, 6380. Sundberg, R. J.; Baxter, E. W. *Tetrahedron Lett.* **1986**, *27*, 2687. Wang, Y.; Lown, J. W. *Heterocycles* **1993**, *36*, 1399. Wang, Y.; Gupta, R.; Huang, L.; Lown, J. W. *J. Med. Chem.* **1993**, *36*, 4172. Tietze, L. F.; Grote, T. *Chem. Ber.* **1993**, *126*, 2733. See also refs 8, 9, and 24.

(26) CBI-based analogs: (a) Boger, D. L.; Munk, S. A. *J. Am. Chem. Soc.* **1992**, *114*, 5487. (b) Boger, D. L.; Yun, W. *J. Am. Chem. Soc.* **1994**, *116*, 5523. (c) Boger, D. L.; Munk, S. A.; Ishizaki, T. *J. Am. Chem. Soc.* **1991**, *113*, 2779. Synthesis: (d) Boger, D. L.; Ishizaki, T.; Wysocki, R. J., Jr.; Munk, S. A.; Kitos, P. A.; Suntornwat, O. *J. Am. Chem. Soc.* **1989**, *111*, 6461. Boger D. L.; Ishizaki, T.; Kitos, P. A.; Suntornwat, O. *J. Org. Chem.* **1990**, *55*, 5823. (e) Boger, D. L.; Ishizaki, T. *Tetrahedron Lett.* **1990**, *31*, 793. (f) Boger, D. L.; Ishizaki, T.; Zarrinmayeh, H.; Kitos, P. A.; Suntornwat, O. *Bioorg. Med. Chem. Lett.* **1991**, *1*, 55. (g) Boger, D. L.; Ishizaki, T.; Sakya, S. M.; Munk, S. A.; Kitos, P. A.; Jin, Q.; Besterman, J. M. *Bioorg. Med. Chem. Lett.* **1991**, *1*, 115. (h) Boger, D. L.; Yun, W.; Teegarden, B. R. *J. Org. Chem.* **1992**, *57*, 2873. (i) Drost, K. J.; Cava, M. P. *J. Org. Chem.* **1991**, *56*, 2240. (j) Aristoff, P. A.; Johnson, P. D. *J. Org. Chem.* **1992**, *57*, 6234. (k) Aristoff, P. A.; Johnson, P. D.; Sun, D. *J. Med. Chem.* **1993**, *36*, 1956.

(27) C_2BI-based analogs: Boger, D. L.; Palanki, M. S. S. *J. Am. Chem. Soc.* **1992**, *114*, 9318. Boger, D. L.; Johnson, D. S.; Palanki, M. S. S.; Kitos, P. A.; Chang, J.; Dowell, P. *Bioorg. Med. Chem.* **1993**, *1*, 27.

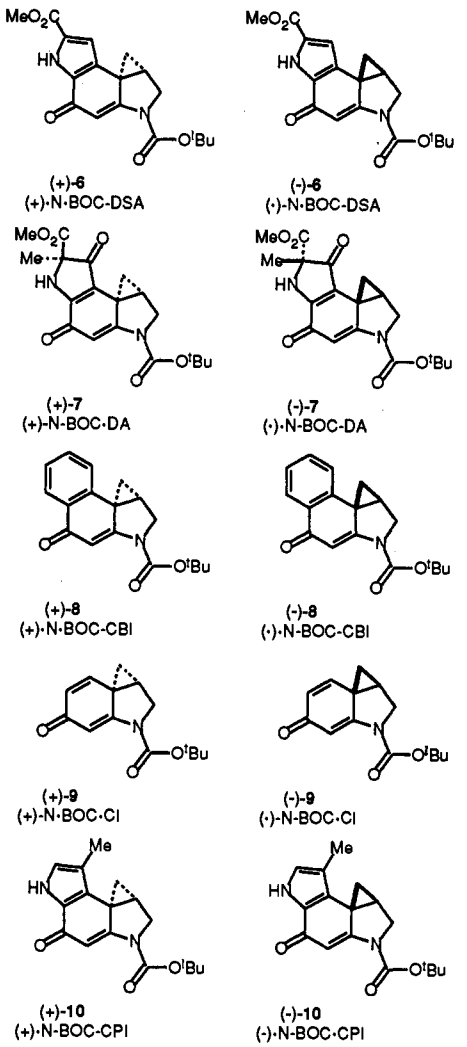

enantiomers was advanced. In these models, the unnatural enantiomers were found to be especially sensitive to steric bulk surrounding the duocarmycin or CPI C7 center by virtue of a significant steric interaction with the alkylated strand 5′ base adjacent to the adenine N3 alkylation site. Because of the diastereomeric relationship of the enantiomer adducts and their reversed binding orientation, the C7 center of the natural enantiomers lies proximal to the complementary strand base which base pairs with the adenine N3 alkylation site and does not suffer a comparable destabilizing steric interaction. Consequently, we have proposed that the unnatural enantiomers are especially sensitive to steric bulk surrounding the duocarmycin C7 center and that as this steric bulk is reduced or removed the distinguishing behavior of enantiomeric pairs of agents diminishes.

Herein, we detail the synthesis and examination of both enantiomers of the CBI analog[26] of the duocarmycins, CBI-TMI (**3**), in efforts to verify two key aspects of the models that have been advanced. On the basis of the relative solvolysis reactivity of **8** and preceding efforts which suggest that there exists a direct, near linear relationship between an agent's solvolysis stability and *in vitro* cytotoxic activity,[13,18,26] we could project that the cytotoxic potency of (+)-CBI-TMI would lie between that of (+)-duocarmycin SA (**1**, L1210 IC_{50} = 10 pM) and (+)-duocarmycin A (**2**, L1210 IC_{50} = 200 pM). In addition because of the inherent steric bulk surrounding the alkylation subunit C8 center in (-)-**3**, we could project that the unnatural enantiomer of CBI-TMI, like the unnatural enantiomer of duocarmycin A (**2**) but unlike those of duocarmycin SA (**1**) and CI-TMI (**4**), would prove to be a significantly less effective DNA alkylating agent and a less potent cytotoxic agent.

Scheme 1

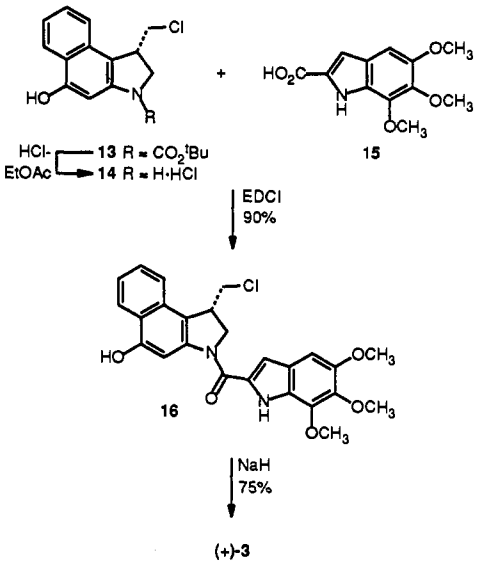

Synthesis of (+)- and (-)-CBI-TMI (3). The precursors **11**–**13** to the CBI alkylation subunit were prepared as disclosed in recent efforts employing a key *5-exo-trig* aryl radical–alkene cyclization for the direct preparation of an appropriately protected 1-(hydroxymethyl)-1,2-dihydro-3*H*-benz[*e*]indole.[26h] However,

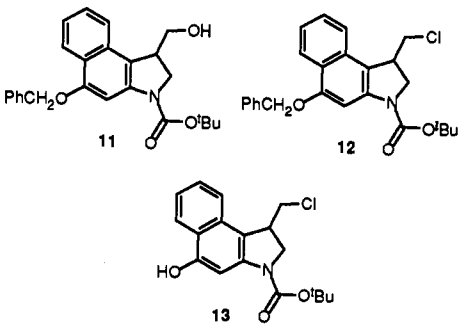

in the course of these and related recent efforts[26b] we have developed a general and improved procedure for the resolution of an advanced synthetic intermediate. In preceding efforts, the resolution was accomplished by esterification of **11** with *(R)*-(-)-*O*-acetylmandelic acid, preparative chromatographic separation of the resulting diastereomers (HPLC 10 μm SiO_2, 10 mm × 25 cm, 1–2% EtOAc–CH_2Cl_2, 2.5–3 mL/min, α = 1.1), and regeneration of the separated enantiomers by hydrolysis of the resolved mandelate esters.[26d,e,28] Although this resolution could be accomplished efficiently, the chromatographic separation of the diastereomers was sufficiently modest (α = 1.1) that it limited the balance of material that could be resolved. In examining alternatives to this diastereomeric derivatization and resolution, we have found that **12** and **13**, more advanced synthetic intermediates than **11**, may be directly and more effectively resolved (α = 1.25–1.37) on analytical and preparative Daicel Chiralcel HPLC columns without recourse to diastereomeric derivatization. Representative results of our studies are summarized in the experimental section. Alcohol **11** could be resolved directly on several Chiralcel columns with excellent α values (1.2–1.37), but only the OD column was found to effectively resolve **11**–**13**. Since **13** is the most advanced synthetic intermediate available, it was selected for preparative resolution. Normal-

(28) Boger, D. L.; Coleman, R. S. *J. Org. Chem.* **1988**, *53*, 695.
(29) Ambrose, C.; Rajadhyaksha, A.; Lowman, H.; Bina, M. *J. Mol. Biol.* **1989**, *210*, 255.
(30) Sanger, F.; Nicklen, S.; Coulsen, A. R. *Proc. Natl. Acad. Sci. U.S.A.* **1977**, *74*, 5463.

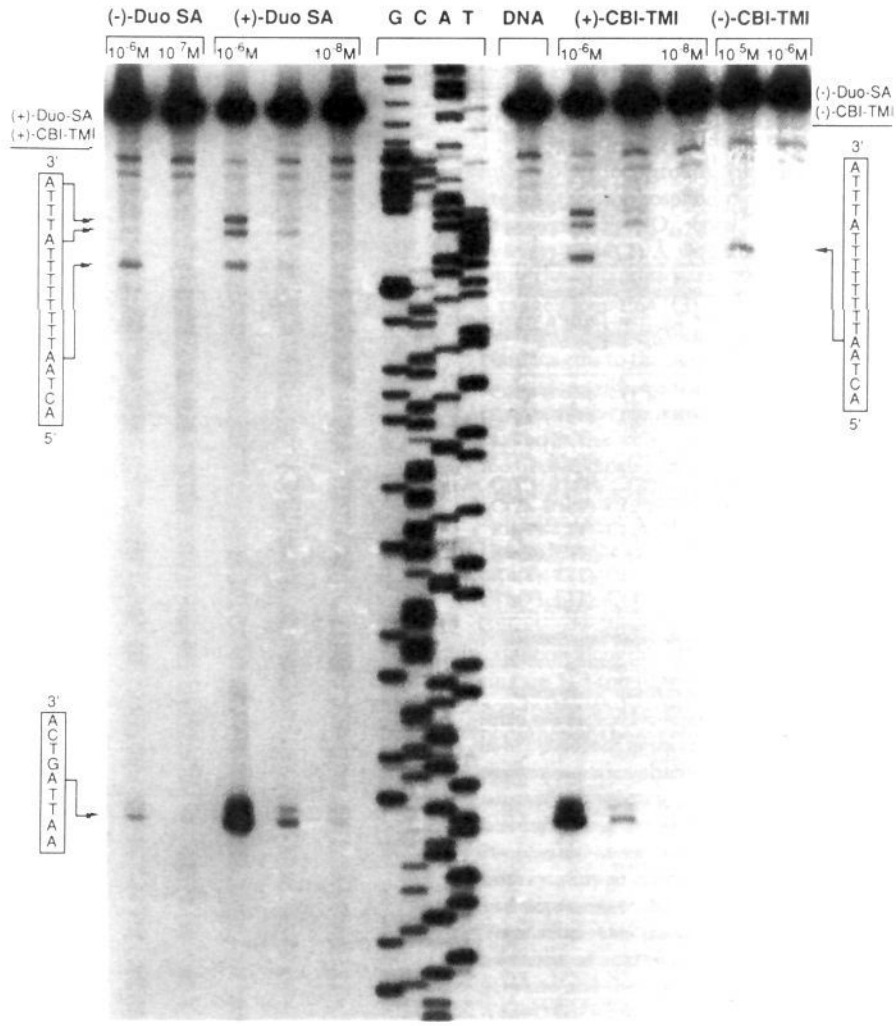

Figure 1. Thermally-induced strand cleavage of 5′ end-labeled duplex DNA (clone w794, 144 bp, nucleotide no. 138-5238). Incubation of agent–DNA at 25 °C (24 h) followed by removal of unbound agent and 30 min thermolysis at 100 °C, denaturing 8% PAGE, and autoradiography. Lanes 1 and 2, *ent*-(−)-duocarmycin SA ((−)-**1**, 1×10^{-6} and 1×10^{-7} M); lanes 3–5, (+)-duocarmycin SA, ((+)-**1**, (1×10^{-6})–(1×10^{-8}) M); lanes 6–9, G, C, A, and T sequencing reactions; lane 10, labeled w794 DNA; lanes 11–13, (+)-CBI-TMI ((+)-**3**, (1×10^{-6})–(1×10^{-8}) M); lanes 14 and 15, *ent*-(−)-CBI-TMI ((−)-**3**, 1×10^{-5} and 1×10^{-6} M). The origin of double bands for a single cleavage site has been detailed elsewhere.[24]

phase preparative chromotography of **13** (2 × 25 cm, 10 μm CHIRALCEL OD column, 8 mL/min flow rate, 5% 2-propanol–hexane, effluent monitored at 254 nm) afforded the two enantiomers: *ent*-(1*R*)-**13** (t_R = 18.2 min) and (1*S*)-**13** (t_R = 23.3 min) (α = 1.28). This resolution, while providing a preparatively useful procedure for the preparation of optically active CBI analogs of CC-1065 and the duocarmycins, has also been found to be of general use for related agents.

Acid-catalyzed deprotection of **13** (3 M HCl–EtOAc, 25 °C, 30 min, 95–100%) and immediate coupling of the unstable indoline hydrochloride salt **14** with 5,6,7-trimethoxyindole-2-carboxylic acid (**15**, 1 equiv)[8] in the deliberate absence of added base[26d] provided the seco-CBI-TMI **16** (91%) in excellent conversion (Scheme 1). Spirocyclization of **16** effected by treatment with NaH (2 equiv, THF–DMF 2:1, 0 °C, 50–60 min, 75%) provided (+)- and (−)-CBI-TMI (**3**) in excellent conversions. Coupling of **14** with **15** in the presence of mild base including $NaHCO_3$ leads to competitive closure of **14** to CBI, lowering the effective yield of amide bond coupling (60–75%), and the presence of adventitious moisture in the spirocyclization reaction mixture leads to subsequent rapid hydrolysis of **3** to **15** and CBI.

DNA Alkylation Properties of (+)- and *ent*-(−)-CBI-TMI (3). The DNA alkylation properties of the agents were examined within five 150 base pair segments of duplex DNA for which comparative results are available for the related agents **1–2** and **4–10**. Five clones of phage M13mp10 were selected for study and contain SV40 nucleosomal DNA inserts: w794 (nucleotide no. 5238-138) and its complement w836 (nucleotide no. 5189-91), c988 (nucleotide no. 4359-4210) and its complement c820 (nucleotide no. 4196-4345), and c1346 (nucleotide no. 1632-1782).[29] The alkylation site identification and the assessment of the relative selectivity among the available sites were obtained by thermally-induced strand cleavage of the singly 5′ end-labeled duplex DNA after exposure to the agents. Following treatment of the end-labeled duplex DNA with a range of agent concentrations (24 h), the unbound agent was removed by EtOH precipitation of the DNA. Redissolution of the DNA in aqueous buffer, thermolysis (100 °C, 30 min) to induce strand cleavage at the sites of DNA alkylation, denaturing high resolution polyacrylamide gel electrophoresis (PAGE) adjacent to Sanger dideoxynucleotide sequencing standards,[30] and autoradiography led to identification of the DNA cleavage and alkylation sites. It has been established in our prior studies that rapid thermolysis at 100 °C at neutral to low pH (pH 6–7) and at low salt concentration minimizes a potentially competitive reversible DNA alkylation reaction and optimizes thermal depurination leading to stoichiometric strand cleavage at the sites of DNA alkylation.[17] Thermal depurination reactions conducted at lower temperatures (50–90 °C), at higher pH (8.0), and to a lesser extent at high ionic strength favor reversal of the DNA alkylation reaction and

Table 1. Consensus Sequence for (+)-CBI-TMI and (+)-Duocarmycin SA DNA Alkylation[a]

base[b]	3	2	1	0	−1	3′
A (30)[c]	57	67	71	100	51	
T (26)	22	33	29	00	18	
G (21)	13	00	00	00	20	
C (23)	08	00	00	00	11	
A/T (56)	79	100	100	100	69	
Pu (51)					71	
consensus	A/T > G/C	A/T	A/T	A	Pu	

[a] Taken from examination of w794/w836, c820/c988, and c1346 DNA. [b] Percentage of the indicated base located at the designated position relative to the adenine N3 alkylation site. [c] Percentage composition within the DNA examined.

result in less efficient strand cleavage. This may be attributed to base-catalyzed phenol deprotonation required for retroalkylation observed at the higher pH or maintenance of duplex (favors retroalkylation) versus denatured (favors depurination) DNA observed at the lower reaction temperatures or at the higher ionic strength. The full details of this procedure have been disclosed and discussed elsewhere.[24]

The statistical treatment of the alkylation sites provided herein proved more revealing than a conventional analysis that considers only the observed alkylation sites. That is, an evaluation that includes the consideration of sites not alkylated helped distinguish the composite consensus sequence and highlighted subtle features not apparent from a simple examination of only the alkylated sites. The DNA alkylation reaction selectivities observed under the incubation conditions of 37 °C (24 h) for the BOC derivatives of the alkylation subunits **6–10** and 4 or 25 °C (24 h) for the natural enantiomers of **1–5** have proven identical to the alkylation selectivities observed with shorter or extended reaction periods (37 or 25 °C, 0.5–7 days). In addition, the selectivity of the DNA alkylation observed under conditions of 25 or 37 °C (24–48 h) for the natural enantiomers of **1–5** has not proven distinguishable from that observed at 4 °C. As discussed in detail below, the unnatural enantiomers of **1** and **3** alkylate DNA at a slower rate and required more vigorous reaction conditions (25 or 37 °C, 24–48 h).

The DNA alkylation selectivities for (+)-CBI-TMI (**3**) and (+)-duocarmycin SA (**1**) were found to be indistinguishable (Figure 1). Each alkylation site detected constituted an adenine flanked by two 5′ A or T bases and there proved to be a preference for this three-base sequence: 5′-AAA > 5′-TTA > 5′-TAA > 5′-ATA. A strong preference but not absolute requirement for the fourth 5′ base to be A or T versus G or C was observed, and this preference distinguished the high-affinity versus low-affinity sites. An additional weak preference for a purine versus pyrimidine base 3′ to the adenine alkylation site was detected and proved more prominent among the low affinity versus high affinity sites. Summarized in Table 1 is the consensus sequence derived from the evaluation of the alkylation sites for (+)-**3**. This fits nicely with the model advanced for (+)-duocarmycin A[12] and (+)-duocarmycin SA[17] of adenine N3 alkylation with agent binding extending in the 3′ → 5′ direction in the minor groove from the alkylation site across an AT-rich 3.5 base pair site.

In addition, (+)-CBI-TMI (**3**) and (+)-**1** were found to alkylate DNA with essentially the same efficiency. For example, the alkylation of w794 DNA illustrated in Figure 1 was detected at 10^{-7} M for both (+)-**1** and (+)-**3** with (+)-**1** alkylating DNA perhaps in a subtly more efficient manner (trace alkylation detected at 10^{-8} M). For practical purposes, this distinction is subtle and probably within error of the experimental protocols. In a more revealing comparison, the relative rate of alkylation of the w794 high-affinity site, 5′-AATTA, was measured (4 °C, 0–24 h) and two agents proved to be nearly indistinguishable: $k(\mathbf{1})/k(\mathbf{3}) = 1.1–1.2$, (Figure 2).

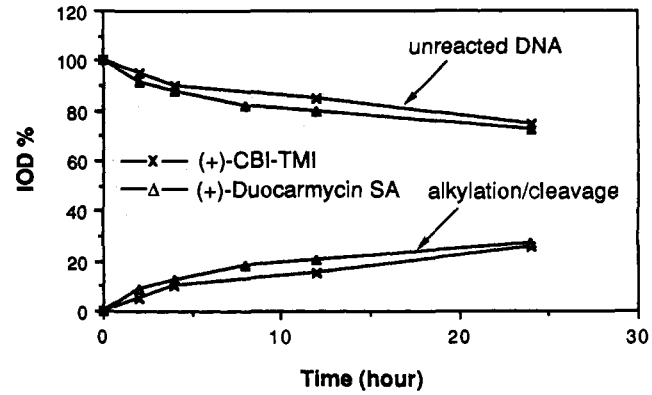

Figure 2. Plot of percent integrated optical density (% IOD) versus time established through autoradiography of 5′ ^{32}P end-labeled DNA and used to monitor the relative rate of w794 alkylation at the 5′-AATTA high-affinity site for (+)-**1** and (+)-**3**.

Table 2. Consensus Sequence for (−)-CBI-TMI and (−)-Duocarmycin SA DNA Alkylation[a]

base[b]	1	0	−1	−2	−3	3′
A (30)[c]	70	100	77	53	35	
T (26)	23	00	19	20	21	
G (21)	00	00	00	17	26	
C (23)	07	00	04	10	18	
A/T (56)	93	100	96	73	56	
consensus	A/T	A	A/T	A/T > G/C	N	

[a] Taken from examination of w794/w836, c820/c988, and c1346 DNA. [b] Percentage of the indicated base located at the designated position relative to the adenine N3 alkylation site. [c] Percentage composition within the DNA examined.

The additional comparisons of the full set of natural enantiomers of **1–4** were even more revealing. Each agent alkylated the same sites within duplex DNA, and the distinctions between the agents lie in their relative efficiency of DNA alkylation and their relative selectivity of alkylation among the available alkylation sites. The least reactive or more stable agents were found to alkylate DNA with both greater efficiency and greater selectivity among the available alkylation sites: (+)-duocarmycin SA (**1**) ≥ (+)-CBI-TMI (**3**) > (+)-duocarmycin A (**2**, 10–100×) > (+)-CI-TMI (**4**, 100–1000×).

In contrast, *ent*-(−)-CBI-TMI (**3**) was found to alkylate DNA only at concentrations approximately 100× that required for (+)-**3** and required more vigorous reaction conditions for its detection (25 °C, 24–48 h). Consequently, (+)-**3** proved to be 100× more effective than (−)-**3** at alkylating DNA. At these higher concentrations, only alkylation derived from the unnatural enantiomer was detected and no alkylation attributable to contaminate natural enantiomer was observed (enantiomeric purity ≥ 99.9%). Consequently, the high affinity alkylation sites unique to the unnatural enantiomer were detected. However, at even higher concentrations (1000–10000×) where the lower affinity sites would be detected, contaminate high affinity alkylation sites attributable to the natural enantiomer became detectable.

Table 2 summarizes the consensus sequence derived from the evaluation of the high-affinity alkylation sites for (−)-**3**, and it was identical to that established for *ent*-(−)-duocarmycin SA.[17] Each alkylation site detected proved to be adenine and essentially each adenine N3 alkylation site was flanked by a 5′ and 3′ A or T base which exhibited the following sequence preference: 5′-AAA > 5′-AAT > 5′-TAA ≥ 5′-TAT. There also was a strong preference for the second 3′ base from the alkylation site to be A or T versus G or C. In this regard, the *ent*-(−)-CBI-TMI alkylation is analogous to that of the natural enantiomer with the exception that the binding orientation is reversed (5′ → 3′) over an AT-rich 3.5 base pair site. However, while the bound

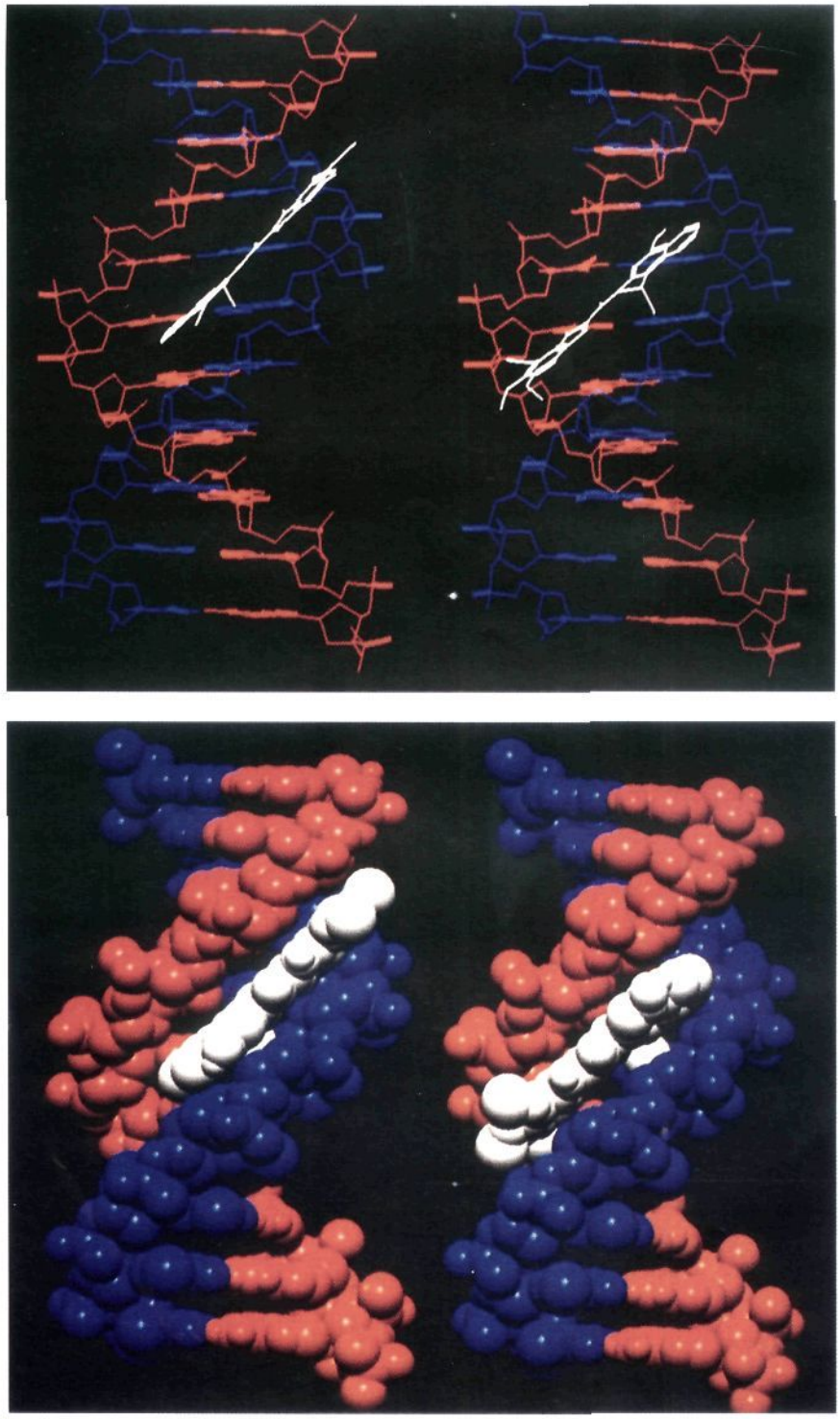

Figure 3. Comparison stick and space filling models of the (+)-CBI-TMI (left) and (–)-CBI-TMI (right) alkylation of a common site within w794 DNA: duplex 5′-(GACTAATTTTT). The natural enantiomer extends in the 3′ → 5′ direction from the adenine N3 alkylation site across the minor site 5′-CTAA. The unnatural enantiomer extends in the reverse 5′ → 3′ direction across the high-affinity site 5′-AATT.

conformation of the natural enantiomer covers an AT-rich 3.5 base pair site extending from the adenine N3 alkylation site in the 3′ → 5′ direction, across the adjacent two to three 5′ bases (*i.e.*, 5′-AAAA), the AT-rich 3.5 base pair site for the unnatural enantiomer extends in the reverse 5′ → 3′ direction, necessarily starting at the first 5′ base site preceding the adenine N3 alkylation site and extending across the alkylation site to the first and second adjacent 3′ bases (*i.e.*, 5′-AAAA). The reversed binding orientation is required to permit the alkylated strand adenine access to the least substituted carbon of the activated cyclopropane, and the offset AT-rich alkylation selectivity is the natural consequence of the diastereomeric relationship of the adducts. Figures 3 and 4 illustrate the (+)- and *ent*-(–)-CBI-TMI models of alkylation within the common w794 5′-(GACTAATTTTT) site which constitutes a high-affinity site for the unnatural enantiomer and a minor site for the natural enantiomer. For (+)-CBI-TMI, the binding spans 3.5 base pairs starting with the 3′ adenine alkylation site and extends in the 3′ → 5′ direction over the 2–3 adjacent 5′ base pairs (5′-CTAA). For (–)-CBI-TMI, the binding similarly spans a 3.5 base pair AT-rich site but which

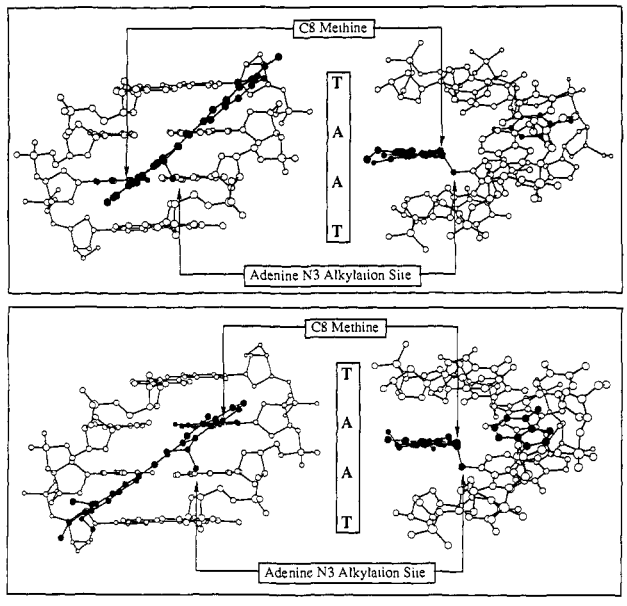

Figure 4. Expanded and rotated minor groove views of the central four base pairs of the (+)-CBI-TMI (top) and (–)-CBI-TMI (bottom) alkylations of the common w794 site of duplex 5′-(GACTAATTTTT) taken from Figure 3. In addition to highlighting the enantiomer reverse binding orientations and offset AT-rich binding sites, the origin of unnatural enantiomer sensitivity to a destabilizing steric interaction between the C8-H and the alkylated strand 5′ adenine adjacent to the alkylation site is highlighted. The natural enantiomer C8-H lies proximal to the complementary strand thymine (in black), which base pairs with the alkylated adenine (C8-H/T C=O = 3.22 Å), while the C8-H of the unnatural enantiomer lies proximal to the alkylated strand 5′ adenine (in black) adjacent to the alkylation site (C8-H/A N3 = 2.02 Å).

starts at the 5′ base adjacent to the alkylation site and extends in the 5′→3′ direction over the alkylation site and the 1–2 adjacent 3′ base pairs (5′-AATT). This offset alkylation selectivity within an AT-rich site is the natural consequence of the diastereomeric relationship of the adducts and the required reversed binding orientation of the agents in the minor groove to permit adenine N3 access to the electrophilic cyclopropane. Presumably the relative importance of the fourth base (A/T > G/C) in the binding sequence is the reason this site constitutes a high-affinity site for the unnatural enantiomer but only a minor site for the natural enantiomer.

The comparison of the unnatural enantiomer series of **1–4** was especially revealing. While *ent*-(–)-duocarmycin A (**2**) did not alkylate DNA,[14] the remaining three agents were found to alkylate the same sites in duplex DNA and the distinctions in the agents lie in their relative efficiency of DNA alkylation and the relative selectivity of alkylation among the available alkylation sites: *ent*-(–)-duocarmycin SA > (–)-CBI-TMI > (–)-CI-TMI ≫ (–)-duocarmycin A. More importantly, the distinctions in the relative efficiency of the natural versus unnatural enantiomer DNA alkylation reactions were found to correlate with the extent of inherent steric bulk surrounding the duocarmycin C7 center: (+)- and (–)-CI-TMI (**4**, 0.5–2×), (+)- and (–)-duocarmycin SA (**1**, 10×), (+)- and (–)-CBI-TMI (**3**, 100×), (+)- and (–)-duocarmycin A (**2**, >100×), (Table 3).

Comparative DNA Alkylation Properties of (+)- and *ent*-(–)-*N*-BOC-CBI. A representative comparison of the DNA alkylation properties of both enantiomers of *N*-BOC-CBI (**8**) and *N*-BOC-DSA (**6**) with (+)-duocarmycin SA is illustrated in Figure 5 with w794 DNA. In addition to illustrating that the DNA alkylation reactions of (+)- and *ent*-(–)-**6** and (+)- and *ent*-(–)-**8** are substantially less efficient (*ca.* 10^4–10^5×) and less selective (selectivity = 5′-AA > 5′-TA), and proceed with an altered profile than either (+)- or (–)-**1** and **3**, both enantiomers of the two simple agents alkylate the same sites. Although these observations

Table 3. Enantiomer Comparisons

agent	rel IC_{50}[a]	rel DNA alkylation[b]
CI-TMI (**4**)	1.0	0.5–2.0
duocarmycin SA (**1**)	10	10
CBI-TMI (**3**)	100	100
duocarmycin A (**2**)	≥110	>100

[a] IC_{50} (L1210) of unnatural(–)/natural(+) enantiomer. [b] Relative concentrations of unnatural(–)/natural(+) enantiomer required to detect w794 DNA alkylation.

may appear unusual, they are the natural consequence of the diastereomeric relationship of the enantiomer adducts. The natural enantiomer binds in the minor groove in the 3′ → 5′ direction from the site of alkylation extending over the adjacent 5′ base. The unnatural enantiomer binds in the reverse 5′ → 3′ orientation but with binding that also covers the same adjacent 5′ base. These alkylation site models which are illustrated in Figures 6 and 7 for (+)- and *ent*-(–)-*N*-BOC-CBI nicely accommodate the observed selectivity of 5′-AA > 5′-TA for *both* enantiomers and highlight the relative sensitivity of the unnatural enantiomer to steric bulk surrounding the CBI C8 center due to a destabilizing steric interaction with the adjacent 5′ base on the alkylated strand. Similar to observations made with **1–4**, the natural enantiomers of **6**, **8–10** were found to alkylate the same sites (5′-AA > 5′-TA) with the more stable agents providing the most efficient and more selective alkylations among the available sites: (+)-*N*-BOC-DSA (**6**) > (+)-*N*-BOC-CBI (**8**, 5×) > (+)-*N*-BOC-CPI (**10**, 25×) > (+)-*N*-BOC-CI (**9**). Although there are subtle distinctions, the unnatural enantiomers of **6** and **8–10** alkylate the same sites as the natural enantiomers and this additional comparison between enantiomeric pairs of agents proved to follow the same observations made with **1–4**. As the inherent steric bulk surrounding the duocarmycin SA C7 or CBI C8 center increases, the relative efficiency of the unnatural versus natural enantiomer alkylation decreases: (+)- and (–)-*N*-BOC-CI (**9**, 1×), (+)- and (–)-*N*-BOC-DSA (**6**, 1×), (+)- and (–)-*N*-BOC-CBI (**8**, 5–10×), (+)- and (–)-*N*-BOC-CPI (**10**, 10–100×). This is nicely illustrated in Figure 5 with w794 DNA, where (+)- and (–)-*N*-BOC-DSA exhibit the same selectivity *and* relative efficiency of DNA alkylation, where (+)- and (–)-*N*-BOC-CBI exhibit the same selectivity of DNA alkylation, but where (+)-*N*-BOC-CBI exhibits a higher efficiency of DNA alkylation than *ent*-(–)-*N*-BOC-CBI (5–10×), and where the (+)-*N*-BOC-CBI DNA alkylation is approximately 5× less efficient than the (+)-*N*-BOC-DSA DNA alkylation reaction. In addition to being more efficient, the (+)- and *ent*-(–)-*N*-BOC-DSA alkylation of DNA proved faster than that of *N*-BOC-CBI and was nearly complete when the reaction was conducted at 37 °C for 24 h, *cf.* lanes 15–18 versus 19–22 of Figure 5. In contrast, the (+)- and *ent*-(–)-*N*-BOC-CBI alkylation reactions were barely perceptible at this point (37 °C, 24 h) and required longer reaction periods for adequate detection (37 °C, 48 h).

Cytotoxic Activity. The *in vitro* cytotoxic activity of (+)- and (–)-CBI-TMI (**3**) proved to be especially interesting. The comparison of (+)-CBI-TMI (**3**) with (+)-duocarmycin SA (**1**), (+)-duocarmycin A (**2**), and (+)-CI-TMI (**4**) was anticipated to provide an additional series of agents in which the relationship between solvolytic stability and biological potency could be directly assessed.[13,18,26] Moreover, the comparison of (–)-CBI-TMI (**3**) with (–)-duocarmycin SA (**1**), (–)-duocarmycin A (**2**), and (–)-CI-TMI (**4**) was expected to provide an additional key series of agents in which the impact of the relative degree of steric bulk surrounding the duocarmycin C7 center on the biological properties of the unnatural enantiomers could be measured.[17,23] Both of these comparisons with the inclusion of the enantiomeric CBI analogs of the duocarmycins proved to be especially important and are summarized in Table 4.

Consistent with expectations, (+)-CBI-TMI (**3**) was found to be an exceptionally potent cytotoxic agent exhibiting an IC_{50} of

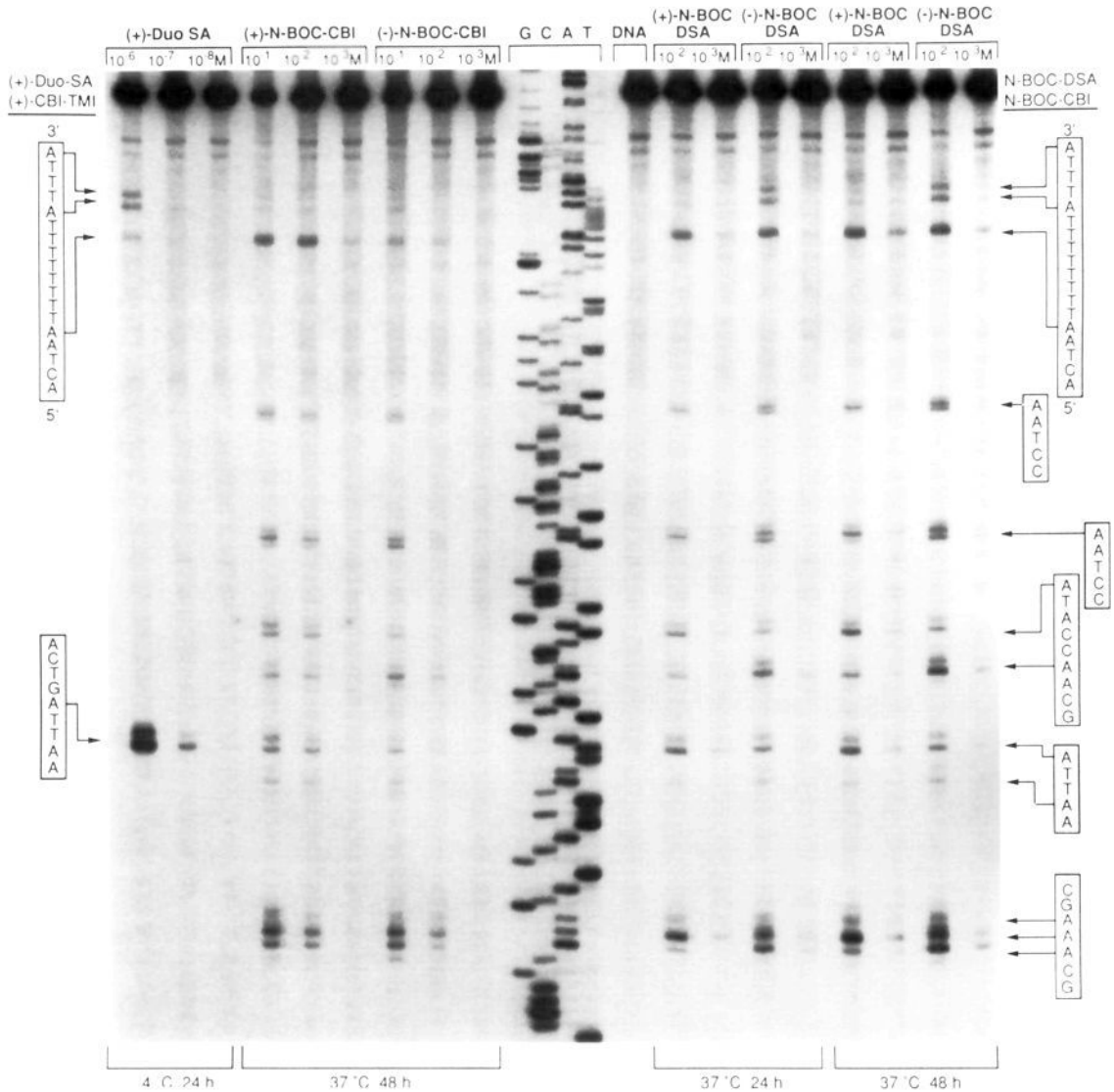

Figure 5. Thermally-induced cleavage of 5′ end-labeled DNA (clone w794, 144 bp, nucleotide no. 138-5238). Unless indicated otherwise the DNA–agent incubation was conducted at 37 °C for 48 h and was followed by removal of unbound agent and 30-min thermolysis at 100 °C, denaturing 8% PAGE, and autoradiography. Lanes 1–3, (+)-duocarmycin SA ((+)-**1**, (1×10^{-6})–(1×10^{-8}) M, 4 °C, 24 h); lanes 4–6, (+)-*N*-BOC-CBI ((1×10^{-1})–(1×10^{-3} M); lanes 7–9, *ent*-(–)-*N*-BOC-CBI ((1×10^{-1})–(1×10^{-3}) M); lanes 10–13, G, C, A, and T sequencing reactions; lane 14, labeled w794 DNA; lanes 15 and 16, (+)-*N*-BOC-DSA ((+)-**6**, (1×10^{-2})–(1×10^{-3}) M, 37 °C, 24 h); lanes 17 and 18, *ent*-(–)-*N*-BOC-DSA ((–)-**6**, (1×10^{-2})–(1×10^{-3}) M, 37 °C, 24 h); lanes 19 and 20, (+)-*N*-BOC-DSA ((+)-**6**, (1×10^{-2})–(1×10^{-3} M); lanes 21 and 22, *ent*-(–)-*N*-BOC-DSA ((–)-**6**, (1×10^{-2})–(1×10^{-3}) M). The origin of double bands for a single cleavage site has been detailed elsewhere.[24]

30 pM (L1210). Consequently, it was determined to be only slightly less potent than (+)-duocarmycin SA (**1**, 10 pM) but substantially more potent than (+)-duocarmycin A (**2**, 200 pM) (Table 4). The relative cytotoxic activity of the natural enantiomers of the full series of agents available to date including (+)-CBI-TMI (**3**) was found to quantitatively follow a well-defined, linear relationship between solvolysis chemical stability and cytotoxic potency. The solvolysis reactivity of the agents established with the simple BOC derivatives of the alkylation subunits *N*-BOC-DSA (**6**),[18] *N*-BOC-CBI (**8**),[26] *N*-BOC-DA (**7**),[31] and *N*-BOC-CI (**9**)[25] follow expectations based on computational studies ($\Delta\Delta H°$, AM1[32])[18] and are summarized in Table 5. Similar to the trend exhibited by the simple BOC derivatives **6–10** (Table 5), the duocarmycin-based agents including (+)-CBI-TMI (**3**) were found to follow a predictable relationship in which the chemically more stable agents exhibit the most potent cytotoxic activity, and this comparison of **1–4** spans 3–4 orders of magnitude (Figure 8). Thus, for agents in a given class which contain the same DNA binding unit (*i.e.*, TMI) and which possess sufficient reactivity to alkylate duplex DNA, this relationship is presumably the consequence of the solvolytically more stable agents more effectively reaching their biological target competitive with nonproductive alkylative or solvolytic consumption in route.

The comparison of the unnatural enantiomers proved even more interesting. (–)-CBI-TMI (**3**) was found to be 100× less potent than (+)-CBI-TMI. Activity at this level was distinguishable

(31) Boger, D. L.; Nishi, T. Unpublished studies. Racemic **7** as a 1:1 mixture of C6 diastereomers was employed for the solvolysis studies reported in Table 5.

(32) Dewar, M. J. S.; Zoebisch, E. G.; Healy, E. F.; Stewart, J. J. P. *J. Am. Chem. Soc.* **1985**, *107*, 902.

(33) This was further verified in the DNA alkylation studies in which a distinct profile of DNA alkylation was observed for *ent*-(–)-CBI-TMI (Figure 1).

(34) In preceding studies,[23,25,26] we have observed similar trends for the cytotoxic activities of both the natural and unnatural enantiomers in additional cell lines. This includes the observation of the natural enantiomer linear relationship between cytotoxic potency and solvolysis stability in B16, P388, KB, and CCRF-CEM cell culture assays although these have not been as extensively examined as L1210.

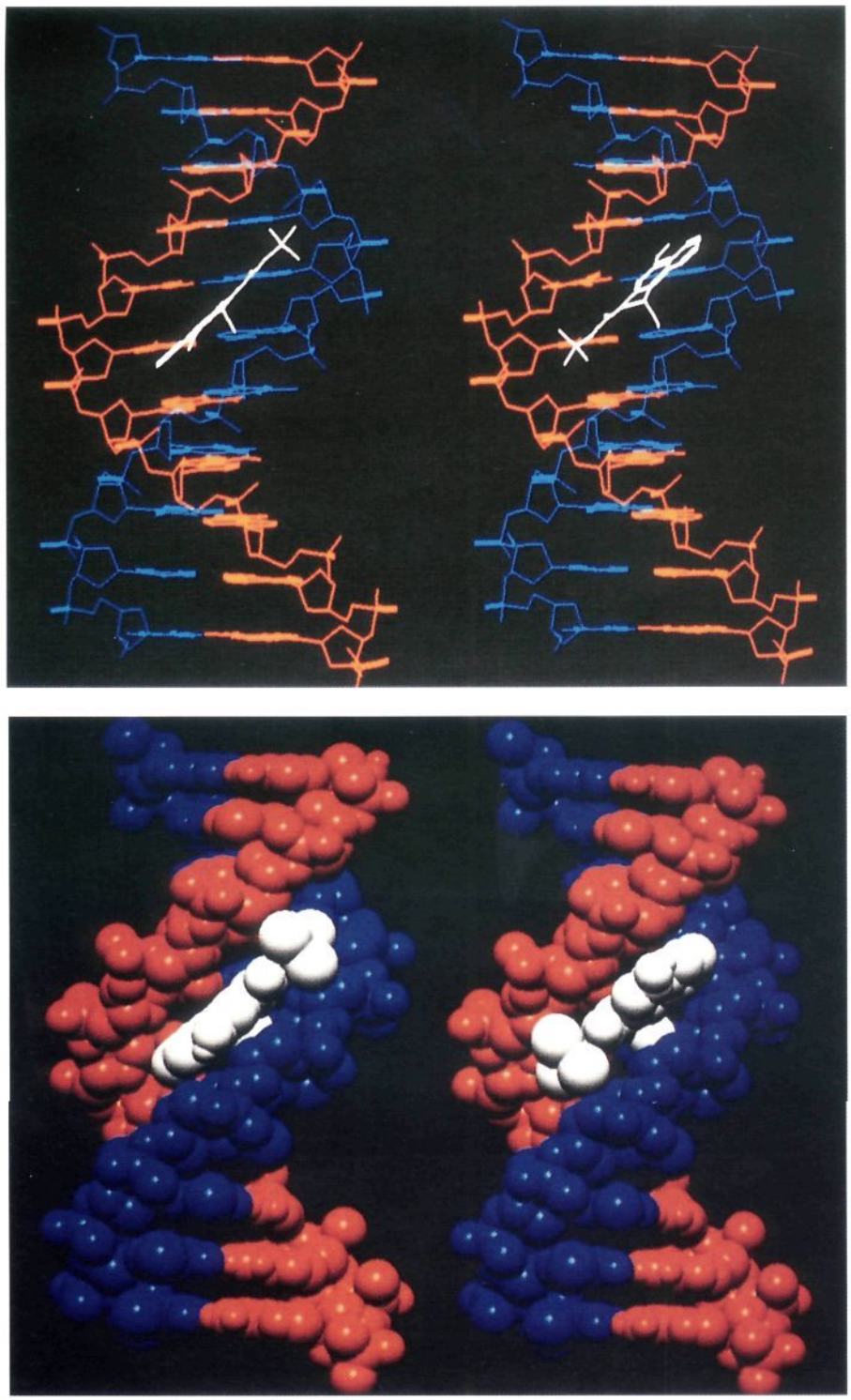

Figure 6. Comparison stick and space filling models of the (+)-*N*-BOC-CBI (left) and *ent*-(−)-*N*-BOC-CBI (right) alkylation of a common w794 DNA site: duplex 5′-(GACTAATTTTT). The natural enantiomer binds in the 3′ → 5′ direction from the adenine N3 alkylation site across the 5′-AA while the unnatural enantiomer binds in the reverse 5′ → 3′ direction but also covers the same 5′-AA site.

from that of potential natural enantiomer contamination of the sample (enantiomeric purity ≥ 99.9%)[33] and fully consistent with the relative DNA alkylation efficiencies observed. In fact, the same trends observed in the distinguishing DNA alkylation properties of the enantiomeric pairs of agents **1–4** were also observed in the relative cytotoxic potencies of the enantiomeric pairs (Table 3).[34]

Conclusions. (+)-CBI-TMI proved essentially indistinguishable from (+)-duocarmycin SA in its ability to alkylate duplex DNA. Its relative efficiency of DNA alkylation was essentially equivalent or perhaps subtly lower, its selectivity of DNA alkylation proved indistinguishable, and its rate of DNA alkylation was only 1.1–1.2× slower in the one direct comparison that was made.

The comparative examination of the full set of natural enantiomers of **1–4** revealed that each agent alkylated the same DNA sites and that the distinctions between the agents lie in their overall relative efficiency of DNA alkylation and their

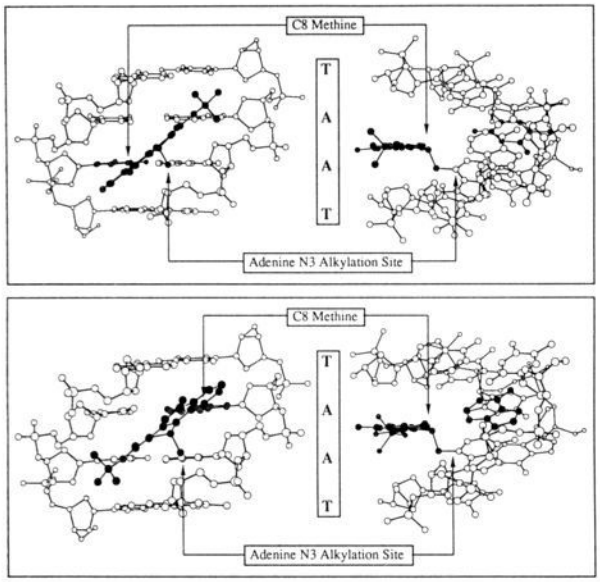

Figure 7. (Top) Expanded and rotated minor groove view of the (+)-*N*-BOC-CBI alkylation of the 5′-AA site taken from the common 5′-(GACTAATTTTT) site in w794 DNA. The natural enantiomer binds in the 3′ → 5′ direction from the adenine N3 alkylation site extending across the 5′-AA site. The C8-H is proximal to the complementary strand thymine (in black) and does not produce a significant destabilizing steric interaction, C8-H/T C=O = 3.17 Å. (Bottom) Expanded and rotated minor groove view of the *ent*-(−)-*N*-BOC-CBI alkylation of the same 5′-AA site in which the unnatural enantiomer binds in the reverse 5′ → 3′ direction but with binding that also covers the same 5′-AA site. The model highlights the unnatural enantiomer sensitivity to destabilizing steric interactions of the C8-H with the alkylation site adjacent 5′ adenine (in black) located on the same strand: C8-H/A N3 = 2.02 Å.

Table 4. *In Vitro* Cytotoxic Activity

agent	configuration	IC_{50} (L1210) pg/mL	pM
(+)-duocarmycin SA ((+)-**1**)	natural	6	10
(+)-CBI-TMI ((+)-**3**)	natural	13	30
(+)-duocarmycin A ((+)-**2**)	natural	100	200
(+)-CI-TMI ((+)-**4**)	natural	10 000	26 000
(−)-duocarmycin SA ((−)-**1**)	unnatural	60	100
(−)-CBI-TMI ((−)-**3**)	unnatural	900	2000
(−)-duocarmycin A ((−)-**2**)	unnatural	≥11 000	≥22 000
(−)-CI-TMI ((−)-**4**)	unnatural	10 000	26 000

Table 5. Solvolysis Reactivity (pH = 3)[a]

agent	k (s^{-1})	$t_{1/2}$	rel $t_{1/2}$	IC_{50}, nM (L1210)[b]	$\Delta\Delta H°$ [d] (kcal/mol)
N-BOC-DSA (**6**)	1.08×10^{-6}	177 h	4.8	6	0
N-BOC-CBI (**8**)	1.45×10^{-6}	133 h	3.6	80	−3.5
N-BOC-CPI (**10**)	5.26×10^{-6}	37 h	1.0	330	−5.8
N-BOC-DA (**7**)	1.75×10^{-5}	11 h	0.3	2000	−9.5
N-BOC-CI (**9**)	1.98×10^{-2}	35 s (5.2 h)[c]	0.001	18 000	−14.8

[a] pH 3: 50% pH 3 buffer–CH_3OH, buffer = 4:1:20 (v/v/v) 0.1 M citric acid, 0.2 M Na_2HPO_4, and H_2O, respectively, measured spectrophotometrically as detailed in ref 18. [b] The natural enantiomer cytotoxic activity. [c] Solvolysis at pH 7 (50% H_2O–CH_3OH); the agents **6**, **8**, and **10** are stable at pH 7 ($t_{1/2}$ > 2 weeks, no UV change). [d] Calculated (AM1) differences in the heats of reaction ($\Delta\Delta H°$) for solvolysis.

relative alkylation selectivity among the available sites. The least reactive and more stable agents alkylated DNA both with greater efficiency and with a greater selectivity among the available sites: (+)-duocarmycin SA (**1**) ≥ (+)-CBI-TMI (**3**) > (+)-duocarmycin A (**2**, 10–100×), > (+)-CI-TMI (**4**, 100–1000×). Similar observations were made with **6–10**.

(−)-CBI-TMI was found to be 100× less effective than (+)-CBI-TMI at alkylating duplex DNA and identical in its sequence

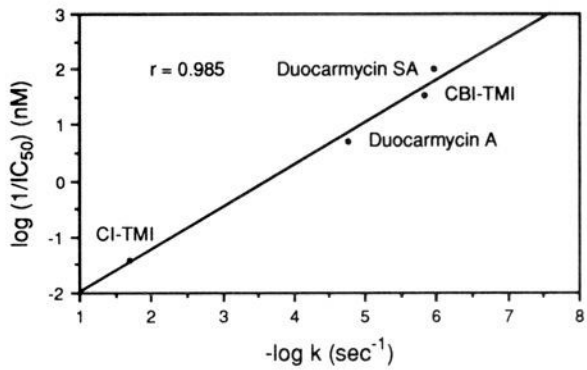

Figure 8.

selectivity with *ent*-(−)-duocarmycin SA (**1**). Importantly, it proved to be 10× less effective at alkylating duplex DNA than *ent*-(−)-duocarmycin SA, consistent with expectations based on recent models which have suggested that the distinguishing relative rate and efficiency of the natural and unnatural enantiomer DNA alkylation reactions may be attributed to the extent of steric bulk surrounding the duocarmycin C7 or CBI C8 center for which the unnatural enantiomers are especially sensitive. The examination of the full set of unnatural enantiomers of **1–4** revealed that while *ent*-(−)- duocarmycin A (**2**) does not alkylate DNA effectively, the remaining three agents alkylate the same duplex DNA sites and that the distinctions among the agents lie in their overall alkylation efficiency and relative selectivity among the available sites: *ent*-(−)-duocarmycin SA (**1**) > (−)-CBI-TMI (**3**) > (−)-CI-TMI (**4**) ≫ *ent*-(−)-duocarmycin A (**2**). More importantly and consistent with recent models, the distinctions in the DNA alkylation efficiencies and biological potencies of pairs of enantiomers were found to correlate exceptionally well with the extent of steric bulk surrounding the duocarmycin C7 or CBI C8 center and, as this steric bulk diminished, the distinguishing relative differences disappeared: (+)- and (−)-CI-TMI (**4**, 0.5–2×), (+)- and (−)-duocarmycin SA (**1**, 10×), (+)- and (−)-CBI-TMI (**3**, 100×), and (+)- and (−)-duocarmcyin A (**2**, >100×).

High-resolution models of the natural and unnatural enantiomer DNA alkylations by **3** and **8** were presented which accommodate the reversed binding orientations, the offset 3.5 base pair AT-rich selectivity, and the distinguishing sensitivity to steric bulk at the duocarmycin C7 or CBI C8 center. The natural enantiomers of **1–4** including **3** alkylate adenine within selected 3–4 base pair AT-rich sites (5′-AAA > 5′-TTA > 5′-TAA > 5′-ATA) with an agent binding orientation that extends in the 3′ → 5′ direction from the site of alkylation covering 3.5 base pairs (*i.e.*, 5′-AAAA). The unnatural enantiomers of **1**, **3**, and **4** similarly alkylate adenine within selected 3–4 base pair AT-rich sites (5′-AAA > 5′-AAT > 5′-TAA > 5′-TAT) but with a binding orientation that extends in the reverse 5′ → 3′ direction covering 3.5 base pairs necessarily starting at the first 5′ base preceding the adenine N3 alkylation site and extending across the alkylation site to the first and second adjacent 3′ bases (*i.e.*, 5′-AAAA). The reversed binding orientation is required to permit a stereoelectronically-controlled adenine N3 addition to the least substituted carbon of the electrophilic cyclopropane, and the offset AT-rich alkylation site selectivity is the natural consequence of the diastereomeric relationship of the adducts.

In contrast, both the natural and unnatural enantiomers of **6–10** including **8** alkylate DNA in a comparable fashion with substantially diminished efficiency (10^4–10^5×), diminished selectivity (5′-AA > 5′-TA), and with a profile that is readily distinguishable from that of either (+)- or (−)-**1–4**. The unusual but general observation that both enantiomers of **8** alkylate the same sites is a natural consequence of the diastereomeric nature of the adenine N3 adducts. The natural enantiomer binds in the minor groove in the 3′ → 5′ direction from the site of alkylation

Table 6

compound	column[a]	eluent (% *i*-PrOH–hexane)	flow rate (mL/min)	α[c]
11	AD	10	1	1.20
	OF	10	1	1.29
	OD	10	1	1.28
	OJ	10	1	ps
	OG	10	1	1.37
	AS	10	1	ps
	OB	10	1	1.0
12	AD	10	1	1.0
	OF	10	1	1.0
	OD	10	1	1.25
	OJ	10	1	ps
	OG	10	1	1.0
	AS	10	1	1.0
	OB	10	1	1.0
13	OD	10	1	1.27
12	OD prep[b]	5	8	1.24
13	OD prep[b]	5	8	1.28

[a] 10 μm, 0.46 × 25 cm analytical column unless noted otherwise. [b] 10 μm, 2 × 25 cm semipreparative column. [c] ps = partial separation.

extending over the adjacent 5′ base while the unnatural enantiomer binds in the reverse (5′ → 3′) but with binding that also covers the same adjacent 5′ base.

Further consistent with expectations, (+)-CBI-TMI (**3**) was found to be an exceptionally potent cytotoxic agent. The full set of natural enantiomers of **1–4** was found to quantitatively follow a well-defined linear relationship between solvolysis stability (functional reactivity) and cytotoxic potency with the more stable agents exhibiting the more potent activity. Presumably, this is a consequence of the solvolytically more stable agents more effectively reaching their biological target competitive with nonproductive consumption in route. Similar observations were made with the agents **6–10**.

Experimental Section

Resolution of 13. 2-Propanol and hexane (Fisher, HPLC grade) were filtered through a Millipore HV filter (pore size = 0.45 μm) and then degassed by stirring under vacuum. A Waters Prep LC 4000 HPLC system equipped with a Daicel Chiralcel OD column (2 × 25 cm, 10 μm) was equilibrated with 5% 2-propanol–hexane at a flow rate of 8 mL/min. Compound **13**[26b] was dissolved in 50% 2-propanol–hexane (150–200 mg/mL), and 100-μL (*ca.* 15 mg) aliquots were injected into the HPLC system at 16–18-min intervals. The effluent was monitored at 254 nm, and the fractions containing resolved **13** were collected: *ent*-(1*R*)-**13** (t_R = 18.2 min) and (1*S*)-**13** (t_R = 23.3 min), α = 1.28. Table 6 summarizes the representative results of a study of the direct resolution of **11–13**.

1-(Chloromethyl)-5-hydroxy-3-[(5,6,7-trimethoxyindol-2-yl)carbonyl]-1,2-dihydro-3*H*-benz[*e*]indole (16, *seco*-CBI-TMI). Phenol **13** (25.0 mg, 0.075 mmol) was treated with anhydrous 3 M HCl–EtOAc (3 mL) at 24 °C for 30 min. The solvent was removed *in vacuo* to afford crude, unstable **14** (quantitative). A mixture of **14**, [3-(dimethylamino)propyl]-ethylcarbodiimide hydrochloride (EDCI, 43.2 mg, 0.2 mmol, 3 equiv), and 5,6,7-trimethoxyindole-2-carboxylic acid (**15**, 18.9 mg, 0.075 mmol, 1 equiv) was stirred in 1.5 mL of DMF at 24 °C under Ar for 6 h. The mixture was diluted with H_2O (1.5 mL) and extracted with EtOAc (3 × 3 mL). The organic layer was washed with 1 N aqueous HCl (1 × 10 mL), saturated aqueous $NaHCO_3$ (1 × 10 mL) and saturated aqueous NaCl (1 × 10 mL), dried (Na_2SO_4), and concentrated. Flash chromatography (0.8 × 10 cm SiO_2, 40–60% EtOAc–hexane gradient elution) afforded **16** (31.8 mg, 35.0 mg theoretical, 91%) as pale-yellow solid: ^{1}H NMR (DMSO-d_6, 400 MHz) δ 11.47 (s, 1H, NH), 10.46 (s, 1H, OH), 8.12 (d, 1H, *J* = 8.0 Hz, C6-H), 7.90 (br s, 1H, C4-H), 7.84 (d, 1H, *J* = 8.0 Hz, C9-H), 7.52 (t, 1H, *J* = 8.0 Hz, C8-H), 7.36 (t, 1H, *J* = 8.0 Hz, C7-H), 7.06 (s, 1H, C3′-H), 6.97 (s, 1H, C4′-H), 4.74 (apparent t, 1H, *J* = 10.4 Hz, C2-H), 4.46 (d, 1H, *J* = 11.2 Hz, C2-H), 4.17 (m, 1H, C1-H), 4.01 (d, 1H, *J* = 10.6 Hz, C*H*HCl), 3.94 (s, 3H, OCH_3), 3.83 (s, 3H, OCH_3), 3.82 (d, 1H, *J* = 11.2 Hz, CH*H*Cl), 3.79 (s, 3H, OCH_3); ^{13}C NMR (DMSO-d_6, 100 MHz) δ 159.8 (C), 153.7 (C), 148.8 (C), 141.8 (C), 139.4 (C), 138.7 (C), 130.7 (C), 129.5 (C), 126.9 (CH), 124.9 (C), 122.8(2CH), 122.7 (C), 122.4 (CH), 121.7 (C), 114.6 (C), 105.7 (CH), 99.8 (CH), 97.6 (CH), 60.7 (CH_3), 60.6 (CH_3), 55.5 (CH_3), 54.7 (CH_2), 47.1 (CH_2), 40.7 (CH); IR (film) ν_{max} 3415, 3190, 2932, 1607, 1582, 1522, 1490, 1448, 1424, 1389, 1311, 1236, 1109 cm^{-1}; FABHRMS (NBA) *m/e* 467.1377 (M^+ + H, $C_{25}H_{23}ClN_2O_5$ requires 467.1374).

Natural (1*S*)-16: $[\alpha]^{23}_D$ –3.1 (*c* 0.13, THF).

***N*²-[(5,6,7-Trimethoxyindol-2-yl)carbonyl]-1,2,9,9a-tetrahydrocyclopropa[*c*]benz[*e*]indol-4-one (3, CBI-TMI).** A suspension of NaH (3.9 mg, 60% dispersion in mineral oil, 0.095 mmol, 2.1 equiv) in THF (1 mL) at 0 °C under Ar was treated with a solution of **16** (21 mg, 0.045 mmol) in 1:1 THF–DMF (2.4 mL), and the reaction mixture was stirred at 0 °C for 1 h. The solvent was removed under vacuo, and the solid residue was diluted with H_2O (10 mL) and extracted with EtOAc (3 × 10 mL). The organic layer then was washed with H_2O (10 mL) and saturated aqueous NaCl (10 mL), dried (Na_2SO_4), and concentrated. Flash chromatography (0.8 × 15 cm SiO_2, 40–60% EtOAc–hexane gradient elution) afforded **3** (14.7 mg, 19.4 mg theoretical, 75%) as a light-tan solid: mp 194 °C (dec); ^{1}H NMR (acetone-d_6, 400 MHz) δ 10.52 (s, 1H, NH), 8.09 (d, 1H, *J* = 7.6 Hz, C5-H), 7.55 (t, 1H, *J* = 7.6 Hz, C7-H), 7.41 (t, 1H, *J* = 7.6 Hz, C6-H), 7.17 (d, 1H, *J* = 8.0 Hz, C8-H), 7.13 (s, 1H, C3′-H), 7.00 (s, 1H, C3-H), 6.93 (s, 1H, C4′-H), 4.61 (dd, 1H, *J* = 5.2, 10.0 Hz, C1-H), 4.50 (d, 1H, *J* = 10.0 Hz, C1-H), 4.00 (s, 3H, OCH_3), 3.86 (s, 3H, OCH_3), 3.85 (s, 3H, OCH_3), 3.16 (m, 1H, C9a-H), 1.76 (dd, 1H, *J* = 8.0, 4.4 Hz, C9-H), 1.68 (d, 1H, *J* = 4.4 Hz, C9-H); ^{13}C NMR (acetone-d_6, 100 MHz) δ 185.6 (C), 162.2 (C), 161.7 (C), 151.2 (C), 142.0 (C), 141.6 (C), 133.7 (C), 132.7 (CH), 130.5 (C), 127.3 (C), 127.1 (CH), 126.8 (CH), 124.4 (C), 123.0 (CH), 111.6 (CH), 108.6 (CH), 108.3 (C), 98.9 (CH), 61.5 (CH_3), 61.4 (CH_3), 56.4 (CH_3), 55.2 (CH_2), 33.3 (C), 28.8 (CH_2), 25.0 (CH); IR (film) ν_{max} 3445, 1645, 1597, 1403, 1302, 1267, 1246 cm^{-1}; FABHRMS (NBA-NaI) *m/e* 431.1610 (M^+ + H, $C_{25}H_{22}N_2O_5$ requires 431.1607).

(+)-3: $[\alpha]^{23}_D$ +218 (*c* 0.49, THF).

***ent*-(–)-3:** $[\alpha]^{23}_D$ –216 (*c* 0.50, THF).

DNA Alkylation Studies of 1, 3, 6, and 8: Selectivity. General procedures, the preparation of singly 5′ end-labeled double-stranded DNA, the agent binding studies, gel electrophoresis, and autoradiography were conducted following procedures described in full detail elsewhere.[24] Eppendorf tubes containing the 5′ end-labeled DNA[24] (9 μL; w794, w836, c820, c988, and c1346 DNA) in TE buffer (10 mM Tris, 1 mM EDTA, pH = 7.5) were treated with the agent in DMSO (1 μL at the specified concentration). The solution was mixed by vortexing the solution and brief centrifugation and subsequently incubated at 4 or 25 °C (**1** and **3**) or 37 °C (**6** and **8**) for 24 h. The covalently-modified DNA was separated from unbound agent by EtOH precipitation and resuspended in TE buffer (10 μL, pH = 7.5). The solution of DNA in an Eppendorf tube sealed with parafilm was warmed at 100 °C for 30 min to induce cleavage at the alkylation sites, allowed to cool to 25 °C, and centrifuged. Formamide dye (0.03% xylene cyanol FF, 0.03% bromophenol blue, 8.7% Na_2EDTA 250 mM) was added (5 μL) to the supernatant. Prior to electrophoresis, the sample was denatured by warming at 100 °C for 5 min, placed in an ice bath, and centrifuged and the supernatant was loaded directly onto the gel. Sanger dideoxynucleotide sequencing reactions[30] were run as standards adjacent to the reaction samples. Polyacrylamide gel electrophoresis (PAGE) was run on an 8% sequencing gel under denaturing conditions (8 M urea) in TBE buffer (100 mM Tris, 100 mM boric acid, 0.2 mM Na_2EDTA) followed by autoradiography.

Relative Rate. Following the procedure detailed above, Eppendorf tubes containing 5′ end-labeled w794 DNA (9 μL) in TE buffer (pH 7.5) were treated with (+)-duocarmycin SA (**1**) or (+)-CBI-TMI (**3**) (1 μL, 10^{-6} M in DMSO). The solutions were mixed and incubated at 4 °C for 2, 4, 8, 12, and 24 h, respectively. Subsequent isolation of the alkylated DNA by EtOH precipitation, resuspension in TE buffer (10 μL, pH 7.5), thermolysis (30 min, 100 °C), concurrent PAGE, and autoradiography were conducted as detailed above. A relative rate of k(+)-**1**/k(+)-**3** = 1.1–1.2 for the alkylation at the w794 high affinity 5′-AATTA site was derived from the slopes of the plots of integrated optical density (IOD) or percent IOD of the high-affinity alkylation site cleavage bands versus time.

Acknowledgment. We gratefully acknowledge the financial support of the National Institutes of Health (Grant CA55276) and we wish to thank Christine M. Tarby for the molecular modeling studies and Figures 3, 4, 6, and 7.